Luminescence and mechanoluminescence of Ba4Si6O16:Eu2+, RE phosphors

Alexis Duval, Yan Suffren, Mourad Benabdesselam, Patrick Houizot, Tanguy Rouxel

▶ **To cite this version:**

Alexis Duval, Yan Suffren, Mourad Benabdesselam, Patrick Houizot, Tanguy Rouxel. Luminescence and mechanoluminescence of Ba4Si6O16:Eu2+, RE phosphors. Journal of Chemical Physics, 2023, 159 (13), pp.134501. 10.1063/5.0167222 . hal-04258645

HAL Id: hal-04258645
https://hal.science/hal-04258645

Submitted on 11 Dec 2023

HAL is a multi-disciplinary open access archive for the deposit and dissemination of scientific research documents, whether they are published or not. The documents may come from teaching and research institutions in France or abroad, or from public or private research centers.

L'archive ouverte pluridisciplinaire **HAL**, est destinée au dépôt et à la diffusion de documents scientifiques de niveau recherche, publiés ou non, émanant des établissements d'enseignement et de recherche français ou étrangers, des laboratoires publics ou privés.

ACCEPTED MANUSCRIPT

The Journal of Chemical Physics

AIP Publishing

This is the author's peer reviewed, accepted manuscript. However, the online version of record will be different from this version once it has been copyedited and typeset.
PLEASE CITE THIS ARTICLE AS DOI: 10.1063/5.0167222

Luminescence and mechanoluminescence of $Ba_4Si_6O_{16}:Eu^{2+}$, *RE* phosphors

Alexis Duval[1,a)], Yan Suffren[2], Mourad Benabdesselam[3], Patrick Houizot[1] and Tanguy Rouxel[1,4]

AFFILIATIONS

[1]Glass Mechanics Lab., IPR (Institut de Physique de Rennes), UMR 6251, University of Rennes, Campus de Beaulieu, Rennes, France.

[2]INSA Rennes, CNRS, ISCR (Institut des Sciences Chimiques de Rennes), UMR 6226, University of Rennes, Campus de Beaulieu, Rennes, France.

[3]INPHYNI (Institut de Physique de Nice), UMR 7010, Côte d'Azur University, Nice, France.

[4]Institut Universitaire de France, Paris, France.

[a)]Author to whom correspondence should be addressed: alexis.duval@univ-rennes.fr

ABSTRACT

The luminescence properties of green $Ba_4Si_6O_{16}:Eu^{2+}$, *RE* (*RE* = Sc, Y, La-Lu except Pm) phosphors are reported. Their long-lasting phosphorescence is discussed in view of trap depths and concentrations determined from thermally stimulated luminescence experiments. A second emission band centered at 439 nm was evidenced at low temperatures, which stems from the substitution of Eu^{2+} in the two non-equivalent Ba^{2+} sites of $Ba_4Si_6O_{16}$. The mechanoluminescence properties of $Ba_4Si_6O_{16}:Eu^{2+}$, *RE* phosphors are described, and a new mechanoluminescence mechanism is proposed, in the case where *RE* = Ho^{3+} involving a trap

distribution from 0.694 to 0.924 eV. Mechanical loading (post UV irradiation) induces a decrease in depth of the trap distribution leading to an increase of the luminescence intensity, whereas a drop of the luminescence intensity is observed upon unloading, following the faster release of the charge carriers.

1. INTRODUCTION

The luminescence properties of oxides, oxynitrides and nitrides from the BaO-SiO_2-Si_3N_4 system were reported in the past few years, such as $BaSi_2O_5$:Eu^{2+} [1] [2] (λ_{em} = 500-505 nm), $Ba_3Si_5O_{13-\delta}N_8$:Eu^{2+} [3] (broad emission bands from 400 to 620 nm), $Ba_5Si_8O_{21}$:Eu^{2+} [4] [5] [6] (λ_{em} = 473-480 nm), $Ba_4Si_6O_{16}$:Eu^{2+} [7] [8] [9] [10] (λ_{em} = 496-515 nm), β-$BaSiO_3$:Eu^{2+} [6] [11] (λ_{em} = 560-565 nm), Ba_2SiO_4:Eu^{2+} [12] [13] [14] [15] (λ_{em} = 503-510 nm), Ba_3SiO_5:Eu^{2+} [6] [16] [17] [18] [19] (λ_{em} = 585-596 nm), $BaSi_2O_2N_2$:Eu^{2+} [20] [21] [22] (λ_{em} = 498-500 nm) or $Ba_2Si_5N_8$:Eu^{2+} [23] (λ_{em} = 585 nm). This chemical system offers a broad range of emission colors, ranging from blue to orange.

The luminescence properties of $Ba_4Si_6O_{16}$:Eu^{2+} were reported as early as the 60s, but were mostly studied during the last 15 years with various luminescent centers such as Eu^{2+}, Pr^{3+} and Ce^{3+} [8] [24] [25]. In the crystal, the rare-earths (*RE*) substitute for Ba^{2+} ions thanks to close ionic radii [26]. Its space group is $P2_1/c$ [27] (a = 12.477 Å, b = 4.685 Å, c = 13.944 Å, β = 93.54°, Z = 2), which is similar to the non-standard $P2_1/a$ formerly used [8]. $Ba_4Si_6O_{16}$:Eu^{2+} is a potential phosphor for applications in white light emitting diodes (*wLEDs*), but synthesis complications including mixed phases like $Ba_3Si_5O_{13}$ and $Ba_5Si_8O_{21}$ and high sintering temperatures limit its use [10].

$Ba_4Si_6O_{16}$ exhibits an intense long-lasting phosphorescence (*LLP*) as well as elastico-mechanoluminescence (*EML*) [28] when doped with Eu^{2+}, in a similar way as $BaSi_2O_2N_2$. Recall that elastico-mechanoluminescence is the emission of light resulting from an elastic

ACCEPTED MANUSCRIPT
The Journal of Chemical Physics
AIP Publishing
This is the author's peer reviewed, accepted manuscript. However, the online version of record will be different from this version once it has been copyedited and typeset.
PLEASE CITE THIS ARTICLE AS DOI: 10.1063/5.0167222

ACCEPTED MANUSCRIPT

The Journal of Chemical Physics

AIP Publishing

This is the author's peer reviewed, accepted manuscript. However, the online version of record will be different from this version once it has been copyedited and typeset.
PLEASE CITE THIS ARTICLE AS DOI: 10.1063/5.0167222

deformation. This phenomenon has recently aroused great interest, because of potential applications of mechanoluminescent materials for energy storage or as stress sensors [29]. The $BaO\text{-}SiO_2$ binary diagram shows a glass-forming region with a BaO content from 20 to 50 mol. % [30], along with congruent crystallization at given BaO contents. This allowed the formation of $Ba_4Si_6O_{16}:Eu^{2+}$, Ho^{3+}-containing glass-ceramics exhibiting *EML* thanks to uniformly dispersed active crystals [28]. In our previous work (ref. [28]), we have reported mechanoluminescence in a new glass-ceramic material mainly consisting of $Ba_4Si_6O_{16}:Eu^{2+}$, *RE* crystalline phase. In this preliminary work, we focused on the choice for the *RE* co-dopant and we have reported the first mechanical testing results, which revealed significant differences with the behavior of $SrAl_2O_4:Eu^{2+}$, Dy^{3+}. The present manuscript provides an in-depth investigation of the role of the co-dopant in the e^- trapping energetics and in the physics of the luminescence mechanism. *LLP* behavior as well as *EML* properties are related to the characteristics of electron traps within the active crystalline phase. Trap depths and concentrations were determined from thermally stimulated luminescence experiments. Experiments with different loading rates and loading modes allow to propose a mechanism of the *EML* phenomenon in the particular crystal.

2. EXPERIMENTAL

$Ba_4Si_6O_{16}:Eu^{2+}$, *RE* crystals were synthesized starting from dried $BaCO_3$ (Sigma-Aldrich 99 %), Gd_2O_3, Lu_2O_3, Dy_2O_3, Sc_2O_3, Eu_2O_3 (Sigma-Aldrich 99.9 %), SiO_2 (Sigma-Aldrich 99.5 %), Pr_2O_3, Sm_2O_3 (Fischer 99.9 %), Tb_4O_7 (Fischer 99.998 %), Tm_2O_3 (Alfa Aesar 99.9 %), Yb_2O_3, La_2O_3, CeO_2, Nd_2O_3 (Rhône-Poulenc 99.99 %), Y_2O_3 (Acros 99.99 %), and Ho_2O_3, Er_2O_3 (Rhône-Poulenc 99.999 %). Three series of $Ba_4Si_6O_{16}:Eu^{2+}$, *RE* crystals were studied, with i) a fixed cationic composition: 35 Ba – 60 Si – 3 Eu – 2 *RE* for each *RE*, ii)

varying Eu^{2+}:*RE* ratio for *RE* = Pr^{3+} or Ho^{3+}, and iii) varying Eu^{2+}+*RE* quantity for *RE* = Ho^{3+}. Stochiometric amounts were weighted and grounded during 15 minutes in ethanol in an agate mortar, and then fired 6 h at 1300 °C in an alumina crucible under a N_2:H_2 = 94:6 reducing atmosphere. Each specimen was grounded into a fine powder.

The X-ray diffraction (*XRD*) patterns were collected using a PANalytical X'pert Pro diffractometer using Cu-Kα radiation (1.5418 Å).

Solid-state excitation and emission spectra were recorded using a Horiba Jobin-Yvon Fluorolog III fluorescence spectrometer equipped with a Xe lamp operating at 450 W, a UV-vis-nearIR photomultiplier (Hamamatsu R928, sensitivity 190 – 860 nm), or a Horiba Jobin-Yvon FluoroMax-4 Plus fluorescence spectrometer equipped with a Xe lamp operating at 150 W and a UV-vis photomultiplier (Hamamatsu R928, sensitivity 190 – 860 nm). The luminescence spectra were realized on powder samples placed inside the solid-sample holder fixed in 30° rotation and blocked by a quartz blade.

Emission and excitation spectra of $Ba_4Si_6O_{16}$:Eu^{2+}, Ho^{3+} were recorded from 77 to 300 K in quartz cuvettes with an optical cryostat (OptistatCF from Oxford Inst.) coupled to a liquid nitrogen bath under a N_2 atmosphere, and from 300 to 380 K in a solid holder using a F-3004 Jobin-Yvon heating Peltier module.

Appropriate filters were used to remove the residual excitation laser light, the Rayleigh scattered light and associated harmonics from the spectra. All spectra were corrected for the instrumental response function.

Solid-state UV-visible absorption measurements were obtained with a PerkinElmer Lambda 650 spectrometer using a 60 mm integrated sphere.

ACCEPTED MANUSCRIPT
The Journal of Chemical Physics
AIP Publishing
This is the author's peer reviewed, accepted manuscript. However, online version of record will be different from this version once it has been copyedited and typeset.
PLEASE CITE THIS ARTICLE AS DOI: 10.1063/5.0167222

Quantum yield measurements were recorded using a G8 GMP integrating sphere according to: $\Phi = (E_c - E_a)/(L_a - L_c)$, where E_c is the integrated emission spectrum of the sample, E_a is the integrated "blank" emission spectrum, L_a is the "blank" absorption, and L_c is the sample absorption at the excitation wavelength. Samples were introduced in specific capillaries for a G8 integrating sphere, and placed directly inside the integrating sphere.

Rapid luminescence decays were measured directly with the fluorescence spectrometer connected to an additional time-correlated single photon counting (*TCSPC*) module and a 360 nm pulsed delta diode. Lifetimes and quantum yields are the averages of three independent measurements.

Luminance, expressed in mcd·m^{-2}, was measured on a 1.5 cm^2 sample pellet using a Konica Minolta LS-150 luminancemeter with an integration time of 3 s under UV irradiation (λ_{exc} = 365 nm) in a lab-made black box. The working distance between the luminancemeter and the pellet surface was 45 cm. The irradiation was realized with a lab-made source constituted by 1 LED CUN66B1B from Roithner at 365 nm plugged in a Keysight Technologies E36104B benchtop power supply that provides the desired current (mA) and voltage (V). The incident beam angle is 30° with respect to the normal of the pellet surface and the distance *LED*-sample is 12 cm. In order to avoid saturation the current was fixed at 90 mA and the voltage at 3.32 V, with an effective power of 0.57 mW·cm^{-2}.

Thermally stimulated luminescence (*TSL*) experiments were performed from 293 to 573 K with a heating rate of 1 K·s^{-1}. The delay between the end of the UV illumination and reading was 40 s. During heating, the *TSL* signal was detected by means of a UV-visible photomultiplier tube.

LLP emission spectra were collected by an optical multichannel analyzer (OMA), consisting of a multimode optical fiber connected to an integrated spectrograph equipped with a CCD array

ACCEPTED MANUSCRIPT
The Journal of Chemical Physics
AIP Publishing
This is the author's peer reviewed, accepted manuscript. However, the online version of record will be different from this version once it has been copyedited and typeset.
PLEASE CITE THIS ARTICLE AS DOI: 10.1063/5.0167222

covering the range 200-1100 nm. An appropriate grating covering the 200-1100 nm range was used.

LLP and *EML* experiments were performed on powder/epoxy composites, where each $Ba_4Si_6O_{16}:Eu^{2+}$, *RE* crystal was mixed with an epoxy resin (obtained by mixing EPOFIX resin Struers and EPOFIX hardener Struers with a 90:10 concentration by weight) with a final powder content of 20 wt. %. Mechanical tests were carried out on disks using a Shimadzu-AGS-X testing machine with a 10 kN load cell and a SiC pusher. The stress σ induced at the center of a disk made in the composite material (epoxy + ceramic powder) during the diametral compression test is expressed as $\sigma = \frac{2P}{\pi dh}$, where P is the load, d the diameter (11.5 mm) and h the height (6 mm) of the disk [31]. The *LLP* intensity and the *EML* intensity were quantified consistently using a Zyla 5.5 sCMOS Andor Technology high sensitivity camera, by irradiating each sample for 2 minutes using a 365 nm handheld UV light with an effective power of 1.22 $mW \cdot cm^{-2}$ prior to mechanical loading.

3. RESULTS AND DISCUSSION

3.1 Luminescence properties of $Ba_4Si_6O_{16}:Eu^{2+}$, *RE*

In a $Ba_4Si_6O_{16}$ crystal, SiO_4 tetrahedra are corner-sharing to form 2-periodic single chains [27] FIG. 1 (a). Three single chains are linked into triple chains, running along [010] with a 2_1 symmetry, therefore forming 6-membered rings [5 7]. Two non-equivalent VIII-coordinated Ba^{2+} sites exist in $Ba_4Si_6O_{16}$, where Ba(1) is located in between two triple chains while Ba(2) is located between two single chains.

Three series of $Ba_4Si_6O_{16}:Eu^{2+}$, *RE* crystals were designed as to study both the incidence of the various *RE* co-doping, the Eu:*RE* ratio and the Eu+*RE* quantity on the luminescence properties.

ACCEPTED MANUSCRIPT
The Journal of Chemical Physics
AIP Publishing
This is the author's peer reviewed, accepted manuscript. However, the online version of record will be different from this version once it has been copyedited and typeset.
PLEASE CITE THIS ARTICLE AS DOI: 10.1063/5.0167222

ACCEPTED MANUSCRIPT
The Journal of Chemical Physics
AIP Publishing
This is the author's peer reviewed, accepted manuscript. However, the online version of record will be different from this version once it has been copyedited and typeset.
PLEASE CITE THIS ARTICLE AS DOI: 10.1063/5.0167222

XRD patterns confirmed the sole crystallization of $Ba_4Si_6O_{16}$ in each sample FIG. 1 (b)**.** The excitation spectra were similar with a change of *RE*, extending up to 420 nm with a maximum at λ_{max} = 329 nm FIG. 2 (a). Just like $Ba_5Si_8O_{21}:Eu^{2+}$, Dy^{3+} [5], such broad excitation spectra make it possible to activate $Ba_4Si_6O_{16}:Eu^{2+}$, *RE* phosphors simply through sunlight irradiation.

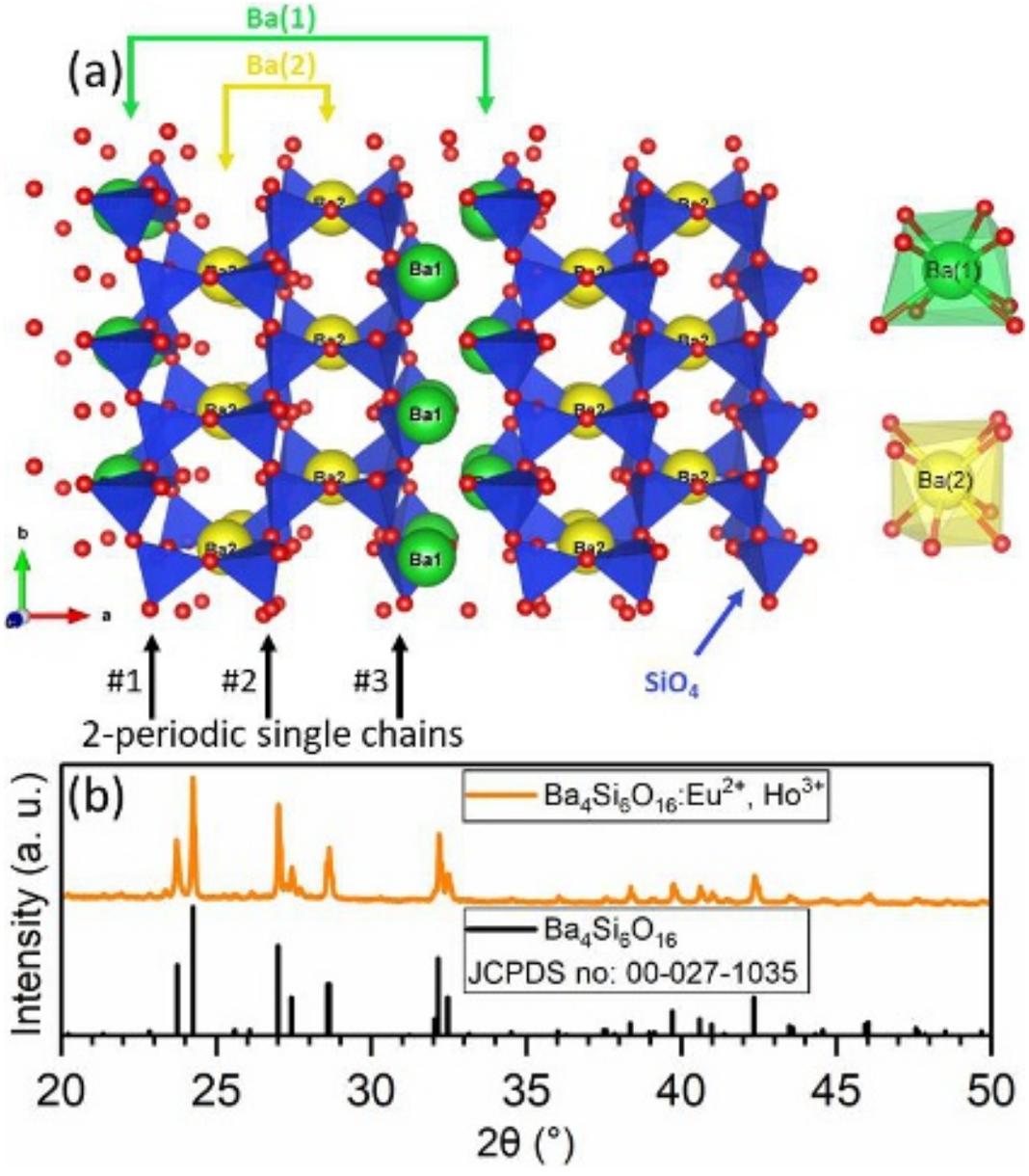

FIG. 1. (a) Crystal structure of $Ba_4Si_6O_{16}$. Green, yellow, and blue polyhedra correspond to Ba(1), Ba(2), and Si-based polyhedra respectively. The local coordination of the Ba(1) and

ACCEPTED MANUSCRIPT
The Journal of Chemical Physics
AIP Publishing
This is the author's peer reviewed, accepted manuscript. However, the online version of record will be different from this version once it has been copyedited and typeset.
PLEASE CITE THIS ARTICLE AS DOI: 10.1063/5.0167222

Ba(2) sites with the oxygen atoms (red) is shown (b) Typical *XRD* pattern of a $Ba_4Si_6O_{16}:Eu^{2+}$, *RE* crystal, here when *RE* = Ho^{3+} (orange), and the standard *XRD* pattern of $Ba_4Si_6O_{16}$ (black).

An excitation wavelength of 365 nm was chosen for the following measurements to remain consistent with the *EML* experiments discussed later in the article. The emission spectra consist of a broad emission band from 400 to 700 nm characteristic of the $4f^65d^1 \rightarrow 4f^7$ transition of Eu^{2+}, with a maximum ranging from 516 to 526 nm. While its position is *RE*-dependent, no conclusions could be obtained regarding its trend. All $Ba_4Si_6O_{16}:Eu^{2+}$, *RE* crystals exhibited a green emission, with CIE coordinates x = 0.302, y = 0.478 when *RE* = Ho^{3+} FIG. 2 (b).

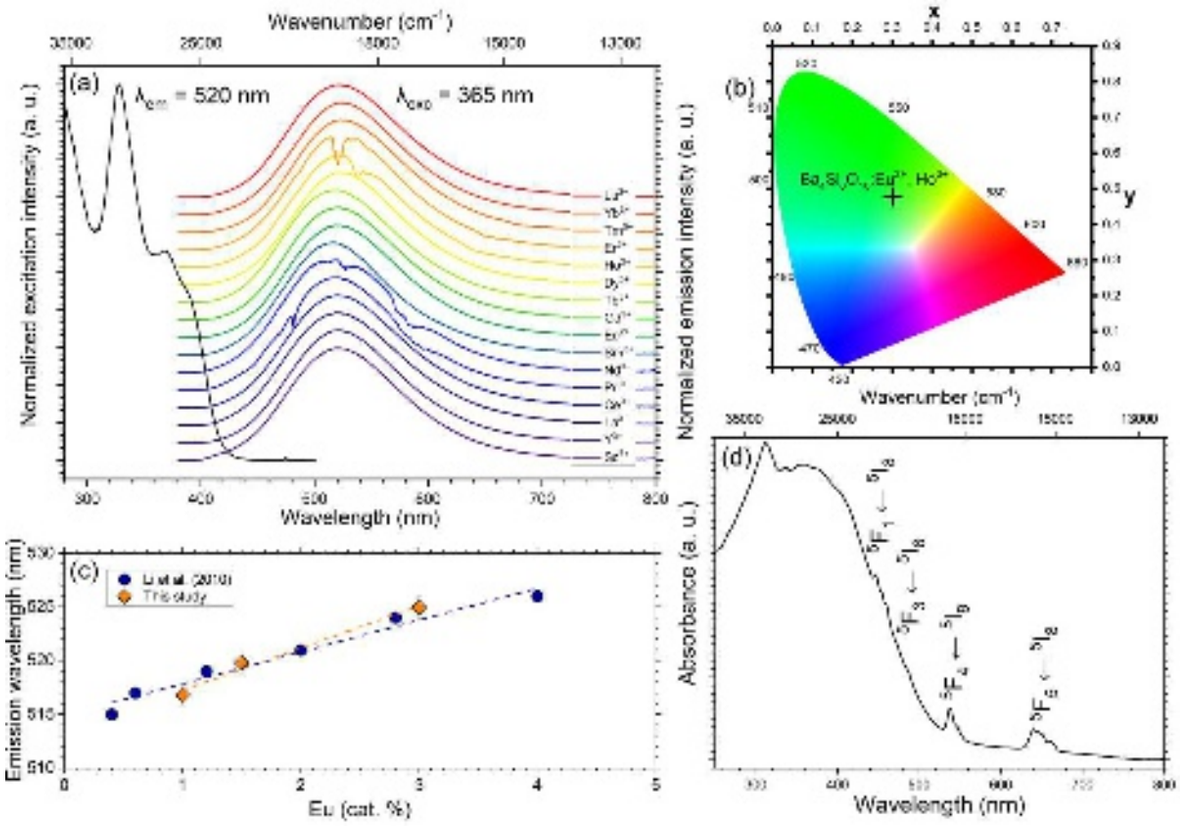

FIG. 2. (a) Excitation spectrum of $Ba_4Si_6O_{16}:Eu^{2+}$, Ho^{3+}, and emission spectra of $Ba_4Si_6O_{16}:Eu^{2+}$, *RE* crystals (b) CIE chromaticity coordinates of $Ba_4Si_6O_{16}:Eu^{2+}$, Ho^{3+} (c) Dependence of the emission wavelength on the europium concentration in $Ba_4Si_6O_{16}:Eu^{2+}$, Ho^{3+}

crystals with a fixed Eu:Ho ratio, and in $Ba_{4-y}Eu_ySi_6O_{15.85}N_{0.1}$ crystals [7] (d) Absorption spectrum of $Ba_4Si_6O_{16}:Eu^{2+}$, Ho^{3+}.

In the literature, the λ_{max} position of the broad emission band of $Ba_4Si_6O_{16}:Eu^{2+}$, *RE* crystals ranges from 494 up to 526 nm. Indeed, its position is slightly redshifted when the europium concentration is increased [7]. Here, the emission maximum of $Ba_4Si_6O_{16}:Eu^{2+}$, Ho^{3+} crystals with a fixed Eu:Ho ratio but with increasing europium concentrations from 1 to 3 cat. % increases from 517 to 525 nm FIG. 2 (c). Typically, Eu^{2+} concentrations from 0.08 to 1.5 cat. % lead to emission maxima ranging from 495 to 505 nm [9 10 32 33], while higher concentrations up to 4 cat. % lead to a maximum emission at 526 nm [7]. Hence, the reported emission color of $Ba_4Si_6O_{16}:Eu^{2+}$, *RE* phosphors ranges from bluish-green to green, and can easily be tuned by choosing the right *RE* co-doping as well as Eu^{2+} concentration. The higher the Eu^{2+} concentration is and the smaller the distance between the europium ions becomes, which means that the probability of energy transfer from higher-energy 5d levels Eu^{2+} ions to lower-energy 5d levels Eu^{2+} ions increases, resulting in the end in an emission band shifting towards longer wavelength [9].

Several absorption peaks were observed when *RE* = Pr^{3+}, Nd^{3+}, Ho^{3+}, or Er^{3+}, with positions at 538, 547, and 638 nm in the case of Ho^{3+} corresponding to transitions from the ground state $^5I_8$ to $^5F_4$, $^5S_2$, and $^5F_5$ respectively [34]. The absorption spectrum of $Ba_4Si_6O_{16}:Eu^{2+}$, Ho^{3+} revealed both the broad absorption band of Eu^{2+} at short wavelength (< 400 nm), as well as various Ho^{3+} intraconfigurational transitions FIG. 2 (d). The absorption and the quantum efficiency were estimated at 79 ± 10 % and 17 ± 10 % respectively with λ_{exc} = 365 nm. Li *et al.* [7] reported a similar absorption (80 %) but a considerably higher quantum efficiency (46 %) in $Ba_{3.8}Eu_{0.2}Si_6O_{15.85}N_{0.1}$.

ACCEPTED MANUSCRIPT
The Journal of Chemical Physics
AIP Publishing
This is the author's peer reviewed, accepted manuscript. However, the online version of record will be different from this version once it has been copyedited and typeset.
PLEASE CITE THIS ARTICLE AS DOI: 10.1063/5.0167222

The luminescence decay was studied over a duration of 6000 ns for *RE* = Ho^{3+} and Er^{3+}. It can be fitted using equation (1):

$$I(t) = A_1 \exp\left(-\frac{t}{\tau_1}\right) + A_2 \exp\left(-\frac{t}{\tau_2}\right) \qquad (1)$$

Where $I(t)$ is the luminescence intensity at a given time t, A_1 and A_2 are constants, and τ_1 and τ_2 are time constants describing the luminescence decay. Two regimes are observed in the beginning for a duration of about 200 s : a rapid one at t < 200 ns followed by a slower one, corresponding respectively to $\tau_1 = 0.107 \pm 0.002$ µs and $\tau_2 = 1.140 \pm 0.004$ µs FIG. 3 (a), suggesting that in both cases the luminescent center is Eu^{2+} while the *RE* act as sensitizers. Yang *et al.* [10] also identified two lifetimes in $Ba_4Si_6O_{16}:Eu^{2+}$, *RE* crystals when *RE* = Eu^{2+}, Dy^{3+}, or Ho^{3+}, however these lifetimes are significantly larger than those reported here (τ_1 = 4 µs and τ_2 = 30.3 µs). In addition, Chen *et al.* [8] observed a decrease of the effective decay time with an increase of the europium content in $Ba_{3.86-y}Si_6O_{16}:0.07Ce^{3+},0.07Li^{+}, yEu^{2+}$, which suggests that a variation of the Eu^{2+}:*RE* ratio and/or Eu^{2+}+*RE* quantity induces a visible change of the specimens lifetime. This was attributed to energy transfers between RE^{3+} co-dopants and Eu^{2+}.

However, the kinetics of the *LLP* decay depends significantly on the selected *RE* FIG. 3 (b). While the steady-state luminescence (*SSL*) intensity is roughly similar whatever the *RE*, the *LLP* intensity changes significantly. For example, it is increased by two orders of magnitude as Ho^{3+} substitutes Sm^{3+}. The *RE* leading to the highest *LLP* intensity at times smaller than 250 s are, in descending order, Ho^{3+} Nd^{3+} Pr^{3+} and Er^{3+}. The luminescence of $Ba_4Si_6O_{16}:Eu^{2+}$, Ho^{3+} is visible to the naked eye beyond a day after the excitation source is stopped. FIG. 3 (c) displays photographs at various times of the *LLP* decay in the case of $Ba_4Si_6O_{16}:Eu^{2+}$, Ho^{3+}.

ACCEPTED MANUSCRIPT
The Journal of Chemical Physics
AIP Publishing
This is the author's peer reviewed, accepted manuscript. However, the online version of record will be different from this version once it has been copyedited and typeset.
PLEASE CITE THIS ARTICLE AS DOI: 10.1063/5.0167222

ACCEPTED MANUSCRIPT
The Journal of Chemical Physics
AIP Publishing
This is the author's peer reviewed, accepted manuscript. However, the online version of record will be different from this version once it has been copyedited and typeset.
PLEASE CITE THIS ARTICLE AS DOI: 10.1063/5.0167222

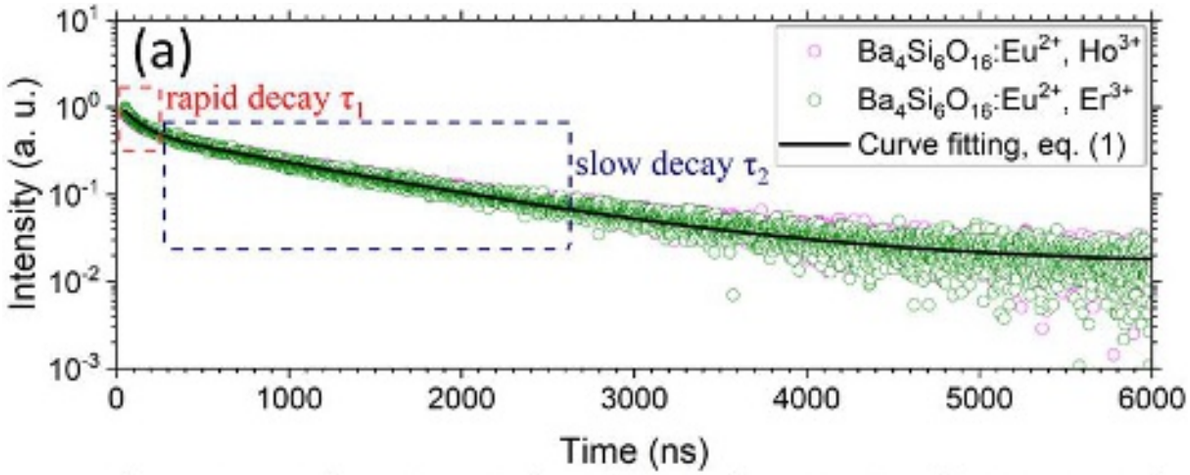

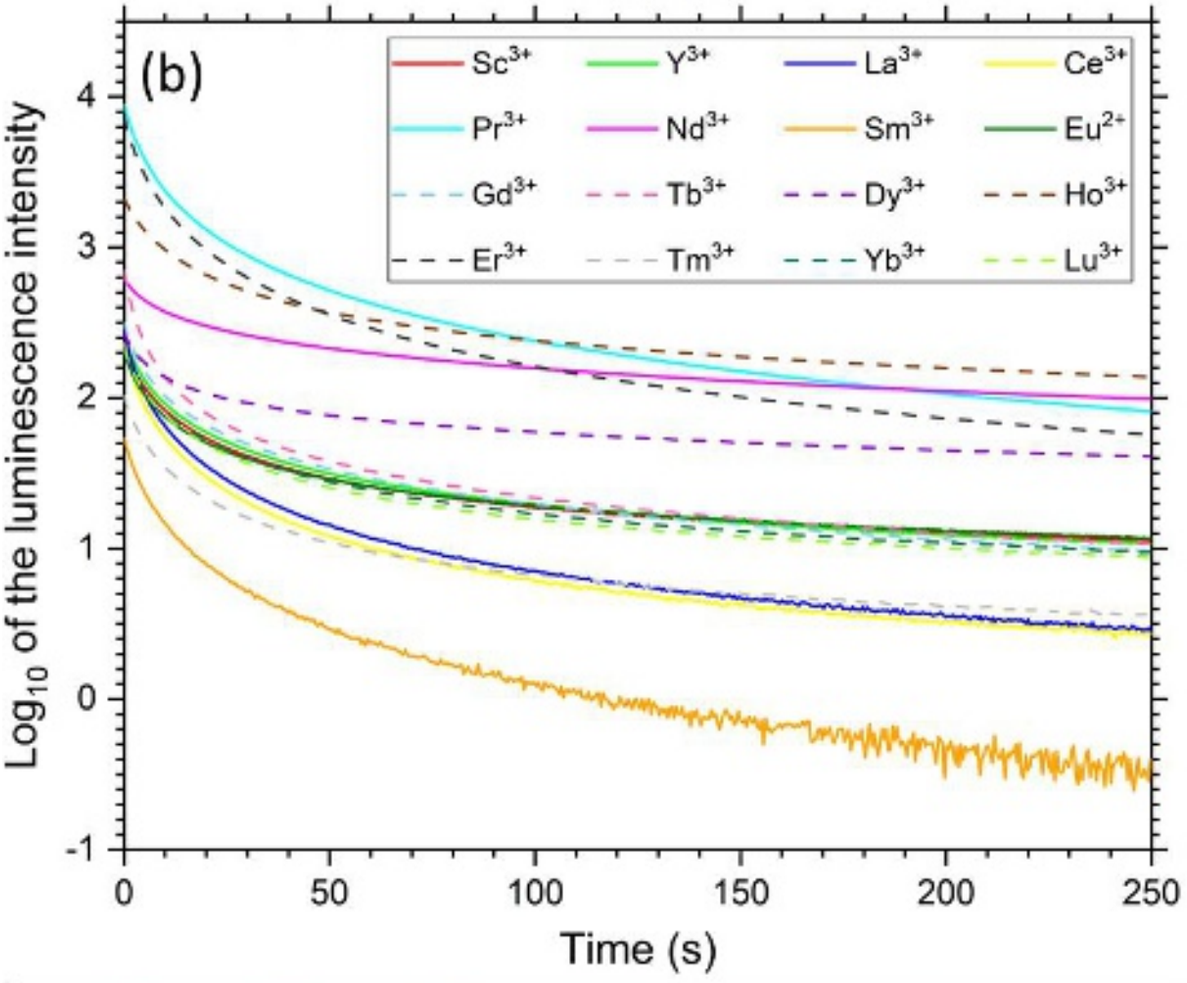

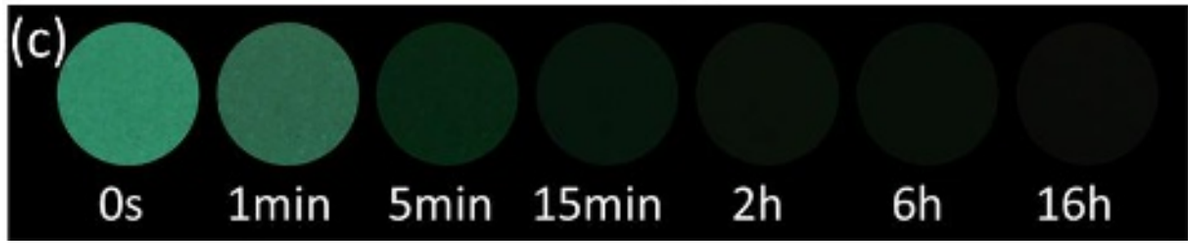

FIG. 3. (a) Rapid-decay of $Ba_4Si_6O_{16}:Eu^{2+}$, *RE* crystals for *RE* = Ho^{3+} or Er^{3+} (b) *LLP* decay of $Ba_4Si_6O_{16}:Eu^{2+}$, *RE* crystals (c) Photographs of $Ba_4Si_6O_{16}:Eu^{2+}$, Ho^{3+} taken at various times after the excitation source is stopped, excited beforehand 2 minutes by a 365 nm UV light. Each disk is 1 cm wide.

The afterglow intensity of $Ba_4Si_6O_{16}:Eu^{2+}$, Ho^{3+} drops by two orders of magnitude as soon as the excitation source is stopped FIG. 4. It is smaller by about 80 % than the one of the well-known $SrAl_2O_4:Eu^{2+}$, Dy^{3+}. Yang *et al.* [10] reported a significantly higher afterglow intensity of $Ba_4Si_6O_{16}:Eu^{2+}$, Ho^{3+}, well above those of previously reported $Ba_4Si_6O_{16}:Eu^{2+}$, *RE* crystals and noticeably stronger than that of $SrAl_2O_4:Eu^{2+}$, Dy^{3+}.

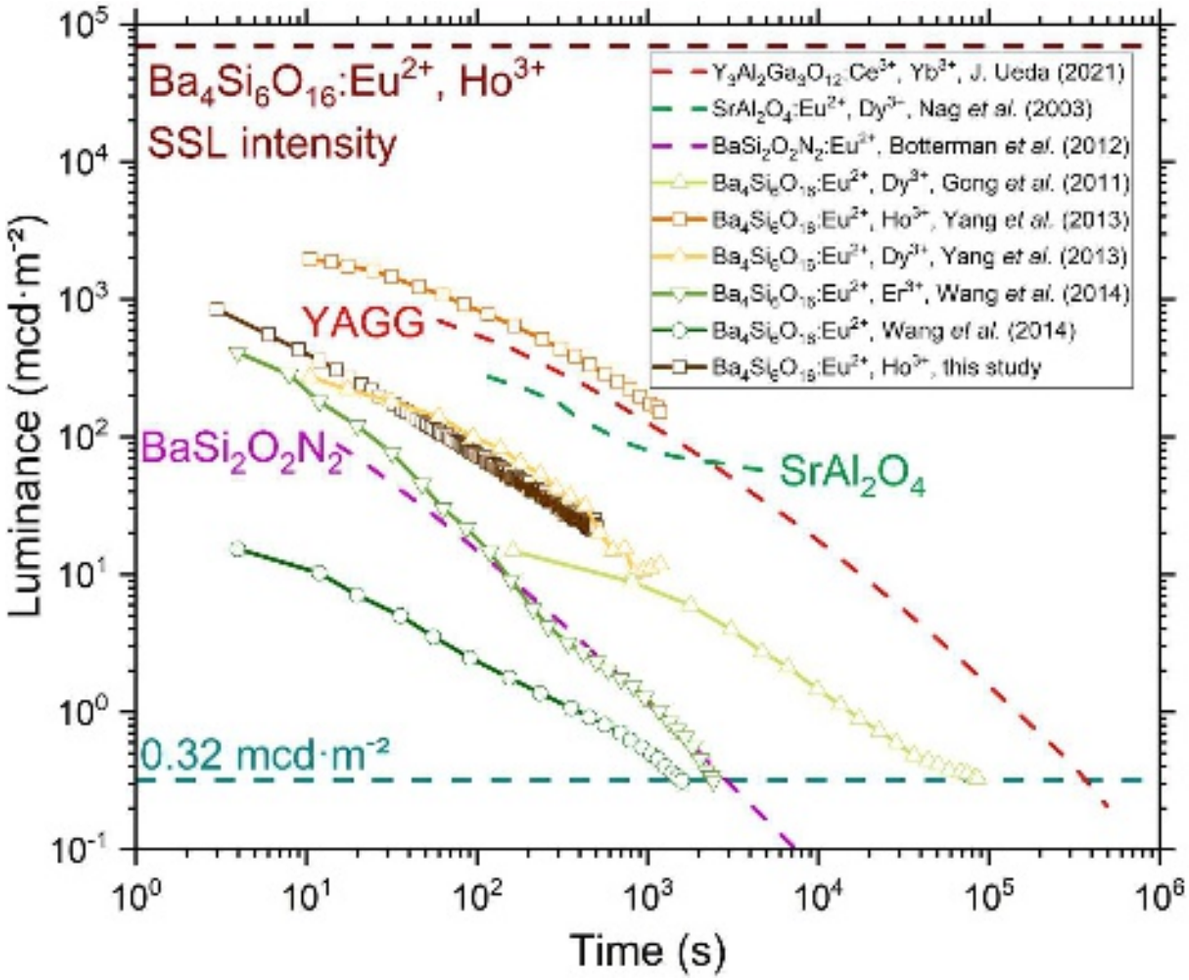

ACCEPTED MANUSCRIPT
The Journal of Chemical Physics
AIP Publishing
This is the author's peer reviewed, accepted manuscript. However, the online version of record will be different from this version once it has been copyedited and typeset.
PLEASE CITE THIS ARTICLE AS DOI: 10.1063/5.0167222

FIG. 4. Luminance of $Ba_4Si_6O_{16}:Eu^{2+}$, *RE* crystals reported here or in the literature [10] [32] [33], as well as that of well-known phosphors such as $Y_3Al_2Ga_3O_{12}:Ce^{3+}$, Yb^{3+} (*YAGG*) [35], $SrAl_2O_4:Eu^{2+}$, Dy^{3+} [36], $BaSi_2O_2N_2:Eu^{2+}$ [37]. The *SSL* intensity of $Ba_4Si_6O_{16}:Eu^{2+}$, Ho^{3+} is also indicated.

TSL experiments provide key elements to better understand the *LLP* intensity and decay, such as the trap depths and distributions. Trap depth E and concentration n_0 can be calculated from the *TSL* intensity $I(T)$ according to [38]:

$$I(T) = \left[\left(\frac{(l-1)s}{\beta}\right) \times \int_{T_0}^{T} \exp\left(-\frac{E}{k_B T}\right) dT + 1\right]^{-\frac{l}{l-1}} s n_0 \exp\left(-\frac{E}{k_B T}\right) \quad (2)$$

Where k_B is the Boltzmann constant, T the temperature, l the kinetic order, s the frequency factor, and β the heating rate (1 $K \cdot s^{-1}$). E, l and s were deduced according to previously described methods [39] [40]. *TSL* curves are plotted in FIG. 5 (a).

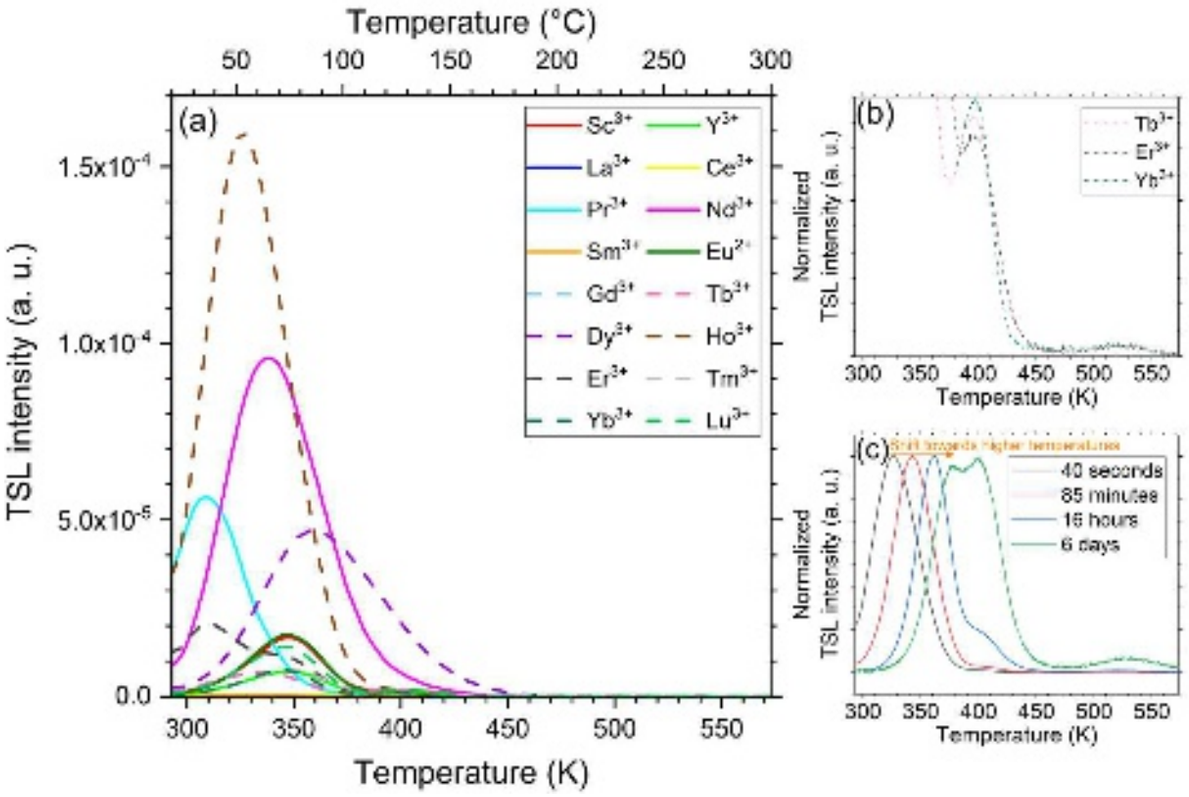

ACCEPTED MANUSCRIPT
The Journal of Chemical Physics
AIP Publishing
This is the author's peer reviewed, accepted manuscript. However, the online version of record will be different from this version once it has been copyedited and typeset.
PLEASE CITE THIS ARTICLE AS DOI: 10.1063/5.0167222

FIG. 5. (a) *TSL* measurements of $Ba_4Si_6O_{16}:Eu^{2+}$, *RE* crystals with a heating rate of 1 $K \cdot s^{-1}$. (b) Zoom-in of the *TSL* measurements highlighting the recurring 398 and 523 K *TSL* peaks (c) *TSL* measurements of $Ba_4Si_6O_{16}:Eu^{2+}$, Ho^{3+} carried out with various delay times.

In $Ba_4Si_6O_{16}:Eu^{2+}$, *RE* crystals, three recurring *TSL* peaks were observed FIG. 5 (a) and FIG. 5 (b). The first one lies in the 303-363 K region, while the second and third ones are systematically located at temperatures of 398 K and 523 K respectively. The only exceptions are i) *RE* = Dy^{3+}, for which the width of the first peak suggests two combined peaks ii) Er^{3+}, which also exhibits two peaks in the 303-363 K region, and iii) Tm^{3+} that exhibits a third peak at 473 K. Such a recurrence in the peak position hints that the nature of those traps is similar regardless of the *RE* co-doping. Further experiments would be required to elucidate the physical and structural origins of these electron traps.

In addition, *TSL* experiments performed with different delay times with *RE* = Ho^{3+} evidenced a gradual shift from the first *TSL* peak towards higher temperatures FIG. 5 (c), which implies that at least for this co-dopant there is actually a distribution of trap depths rather than a discrete energy level. This is consistent with preliminary *DFT* calculations performed on the $Ba_4Si_6O_{16}$ crystal, which also show the presence of a distribution of energy levels arising from oxygen vacancies [28]. This distribution of energies would extend from at least $E_{C_3} = 0.694$ to $E_{C_1} = 0.924$ eV, where C_3 is the top and C_1 the bottom of the trap distribution. It is slightly shallower than that reported by Yang *et al.* (which extended from 0.602 to 1.156 eV) [10], where its deepness was possibly overestimated because of the close second *TSL* peak at 398 K. As a matter of fact, short (< 500 s) and long time (up to 60000 s) luminescence decay measured at the peak emission wavelength would suggest that this distribution is close to a gaussian form FIG. 6 [41] [42] [43] [44]. It is noteworthy that *RE* co-doping in $Ba_4Si_6O_{16}$ does not always lead to a

ACCEPTED MANUSCRIPT
The Journal of Chemical Physics
AIP Publishing
This is the author's peer reviewed, accepted manuscript. However, the online version of record will be different from this version once it has been copyedited and typeset.
PLEASE CITE THIS ARTICLE AS DOI: 10.1063/5.0167222

ACCEPTED MANUSCRIPT
The Journal of Chemical Physics
AIP Publishing
This is the author's peer reviewed, accepted manuscript. However, the online version of record will be different from this version once it has been copyedited and typeset.
PLEASE CITE THIS ARTICLE AS DOI: 10.1063/5.0167222

distribution of trap depths. For example, Dy^{3+} co-doping does not induce a shift of the first *TSL* peak position with increasing delay times [10].

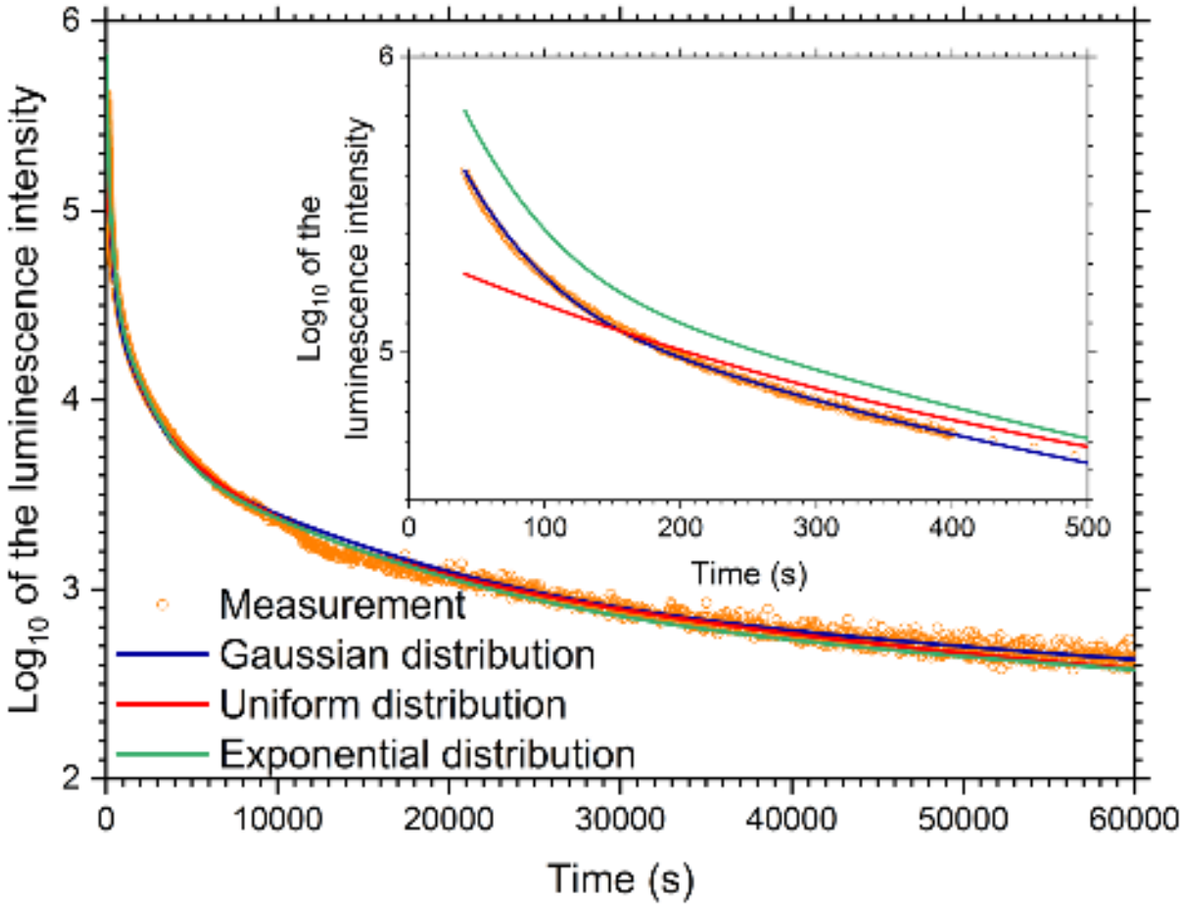

FIG. 6. *LLP* decay (< 60000 s) of $Ba_4Si_6O_{16}:Eu^{2+}$, Ho^{3+} fitted with various distribution shapes. The inset shows the *LLP* decay at short times (< 500 s).

In order to get more insight into the *LLP* behavior of $Ba_4Si_6O_{16}:Eu^{2+}$, *RE* crystals at the scale of a few minutes, only traps with a depth of 1 eV at most need to be considered, which correspond to the first peak in the 303-363 K region. Thus, the second and third peaks, which correspond to deeper traps are excluded from this study. The high sensitivity camera used for *LLP* experiments does not allow to quantify the luminescence intensity immediately after the excitation source is stopped. Therefore, the luminescence intensity at an arbitrarily chosen time of 250 s was used as a reflection of the *LLP* lifetime. As can be seen in FIG. 7, there is an

ACCEPTED MANUSCRIPT
The Journal of Chemical Physics
AIP Publishing
This is the author's peer reviewed, accepted manuscript. However, the online version of record will be different from this version once it has been copyedited and typeset.
PLEASE CITE THIS ARTICLE AS DOI: 10.1063/5.0167222

excellent agreement between the *LLP* behavior and the traps depths and concentrations as determined from the spectra in FIG. 5 by means of equation (2): the $Ba_4Si_6O_{16}:Eu^{2+}$, *RE* crystals with the strongest afterglow intensity are the ones with the largest concentrations of traps with depths ranging from 0.65 to 0.85 eV, a region where the relaxation kinetics to the fundamental state is of the order of a few minutes to several days.

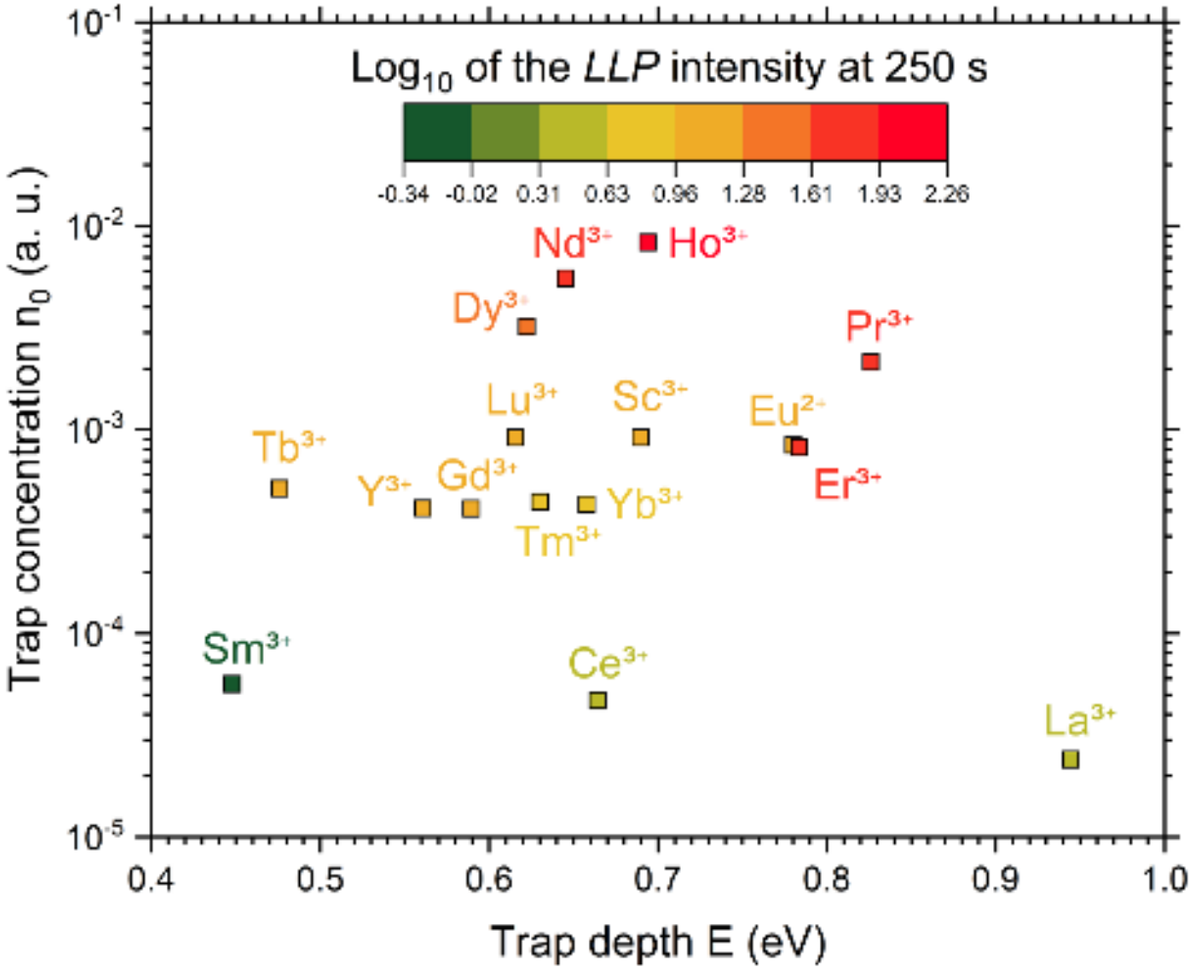

FIG. 7. Trap depth and concentration of the various $Ba_4Si_6O_{16}:Eu^{2+}$, *RE* crystals determined from equation (2).

ACCEPTED MANUSCRIPT

The Journal of Chemical Physics

AIP Publishing

This is the author's peer reviewed, accepted manuscript. However, the online version of record will be different from this version once it has been copyedited and typeset.
PLEASE CITE THIS ARTICLE AS DOI: 10.1063/5.0167222

3.2 Eu(1) and Eu(2) emission bands

As europium ions are incorporated in $Ba_4Si_6O_{16}$ crystals, Eu^{2+} will occupy the two non-equivalent Ba^{2+} sites. It was proposed that, because both Ba(1) and Ba(2) sites are coordinated by eight oxygen atoms [27], the two europium ions environments are relatively similar, in agreement with the fact that two broad emission bands with close emission maximum are observed [7 10 32]. Indeed, while the 4f electrons of divalent europium are quite insensitive to their surroundings, this is not the case of the 5d electrons [32]. Consistently, the broad emission band could be deconvoluted into two bands at λ_{max} = 500 and 550 nm, corresponding to the two non-equivalent europium sites, namely Eu(1) and Eu(2) [32]. This is supported by i) a shift of the broad emission band maximum towards longer wavelength when the delay time increases, which suggests the existence of two different lifetimes for each site [32], and ii) a significantly different excitation spectra when λ_{em} = 500 or 550 nm.

Thermoluminescence experiments performed in this work from 77 to 380 K support another interpretation. When the emission spectra are measured at temperatures as low as 77 K, one can observe a second emission band appearing at λ_{max} = 439 nm, in addition to the green emission band at λ_{max} = 521 nm FIG. 8 (a). The intensity of this blue emission band gradually decreases up to 200 K where it is no longer visible, while the thermal quenching of the green emission band starts at 160 K but is not yet completed at 380 K. Furthermore, excitation spectra collected at 77 K with λ_{em} = 500, 521, or 550 nm are identical FIG. 8 (b), but all-three were notably different from the one obtained with λ_{em} = 439 nm. Indeed, the latter is shifted towards shorter wavelengths and its behavior in the 330-400 nm region is clearly unalike. This is in contradiction with what was previously reported [32]. This suggests that i) the blue and green emission bands are of different nature, which is clearly outlined when λ_{exc} = 312 nm, and ii) the green emission band is not composed of two subsequent emission bands.

ACCEPTED MANUSCRIPT

The Journal of Chemical Physics

AIP Publishing

This is the author's peer reviewed, accepted manuscript. However, the online version of record will be different from this version once it has been copyedited and typeset.
PLEASE CITE THIS ARTICLE AS DOI: 10.1063/5.0167222

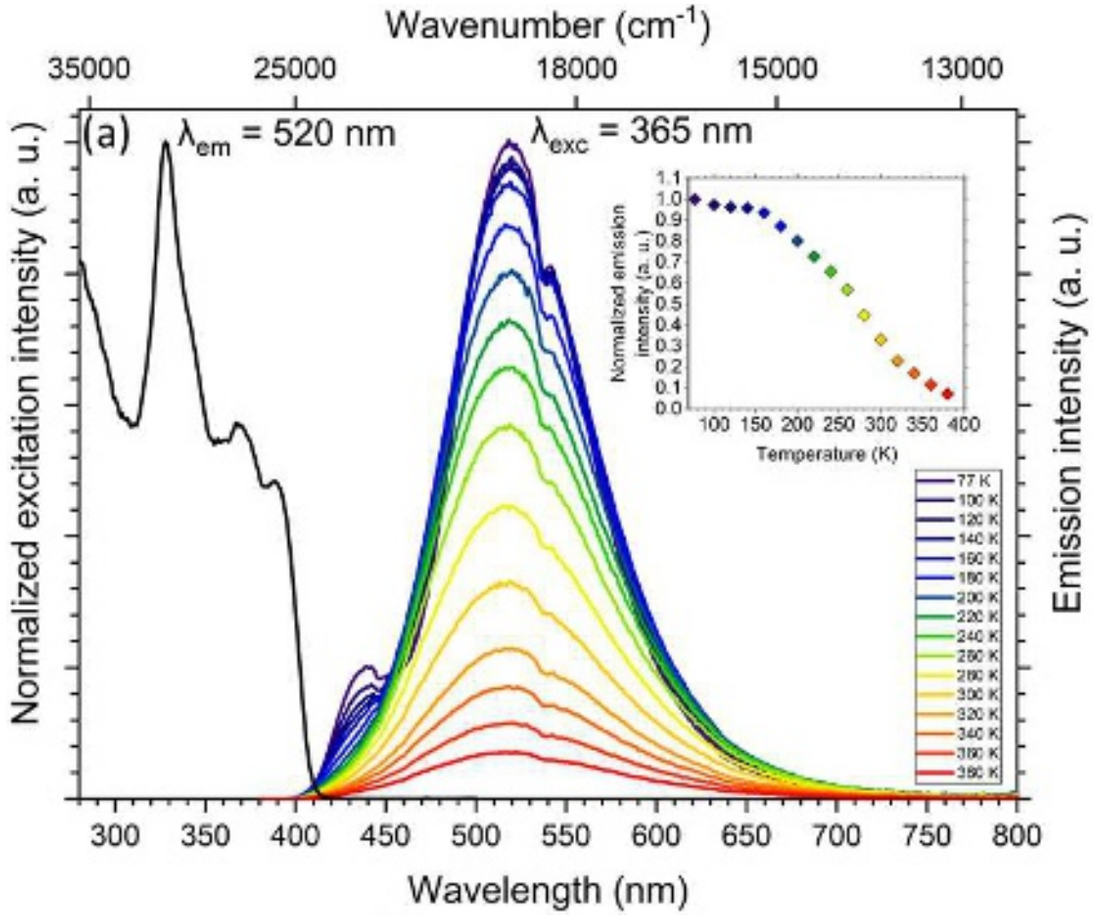

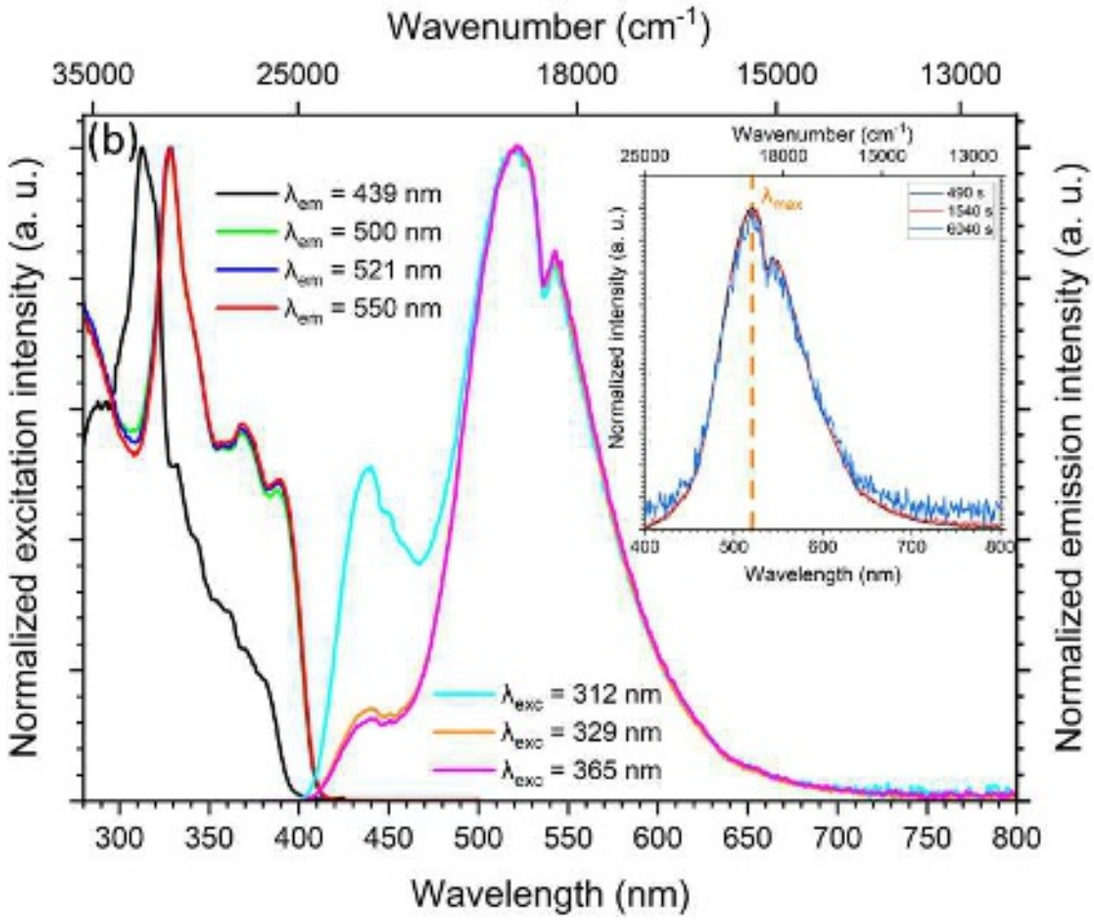

FIG. 8. (a) Excitation spectra measured at 77 K and emission spectra measured at various temperatures (20 K steps) of $Ba_4Si_6O_{16}:Eu^{2+}$, Ho^{3+}. The inset shows the emission intensity at various temperatures. (b) Excitation and emission spectra of $Ba_4Si_6O_{16}:Eu^{2+}$, Ho^{3+} at 77 K. The inset shows the *LLP* emission spectra at ambient temperature various times after the excitation source is stopped.

The interpretation proposed in this work is supported by emission spectra measured at various times after the excitation source is stopped, where no shift of the emission maximum was observed FIG. 8 (b), which was already noted in another study [45]. The previously observed shift is likely resulting from the presence of β-$BaSiO_3$ as a secondary phase, which is revealed by the presence of a peak on the *XRD* pattern at 26° FIG. 1. The persistent luminescence properties of this crystal are known [11] and an emission maximum at λ_{max} = 560 nm was identified, which explains the shift of the emission maximum towards longer wavelengths with time.

It is thus concluded that the two non-equivalent Eu^{2+} sites are sufficiently different to give birth to two emission bands at low temperatures. Indeed, the Ba(1) polyhedron is more distorted than the Ba(2) one [27], so that an 82 nm difference between the two emission bands maximum is observed. It was proposed that the higher distortion degree of the Ba(1) polyhedra would result in a weaker crystal field of Ba(1) than that of Ba(2) [10], thus, the broad emission band of Eu(1) would be in a shorter wavelength region than that of Eu(2) [46], *i. e.* the blue emission band would correspond to Eu(1) and the green one to Eu(2). However, it is still not clear as to why the thermal quenching of Eu(1) occurs at much lower temperatures than that of Eu(2).

The thermoluminescence behavior of $Ba_4Si_6O_{16}:Eu^{2+}$, Ho^{3+} is very similar to that of monoclinic $SrAl_2O_4:Eu^{2+}$, Dy^{3+}. In the latter, a blue emission band also appears at low temperatures (λ_{max} = 445 nm) which arises from the presence of two non-equivalent Sr^{2+} sites in the crystal structure [47]. In addition, the asymmetric green emission band of $Ba_4Si_6O_{16}:Eu^{2+}$, Ho^{3+} is shifted

ACCEPTED MANUSCRIPT
The Journal of Chemical Physics
AIP Publishing
This is the author's peer reviewed, accepted manuscript. However, the online version of record will be different from this version once it has been copyedited and typeset.
PLEASE CITE THIS ARTICLE AS DOI: 10.1063/5.0167222

to larger wavelengths just like the green emission band (λ_{max} = 520 nm) of strontium aluminate. In this latter case, this was discussed by Botterman *et al.* [47] in terms of the centroid shift and crystal field splitting.

3.3 Mechanoluminescence properties of $Ba_4Si_6O_{16}:Eu^{2+}$, *RE*

The *EML* response of $Ba_4Si_6O_{16}:Eu^{2+}$, *RE*/epoxy composites, obtained by subtracting the *LLP* intensity as recorded at rest (*i. e.* at σ = 0 MPa) to the mechanically-loaded specimen, was characterized by means of the diametral compression tests FIG. 9 (a). Each test was performed with a 0.37 $MPa \cdot s^{-1}$ stress rate. It is recalled that the *EML* intensity is proportional to both the stress and the stress rate [48]. In a similar way as with the previous *LLP* measurements, the *RE* co-doping has a pronounced effect on the intensities of the *EML* signal. The largest intensities are obtained with *RE* = Ho^{3+}, Pr^{3+}, Er^{3+}, or Nd^{3+} FIG. 9 (b). The mechanical stress was applied 90 s after the excitation source was stopped, as longer delays resulted in smaller *EML* intensity. This suggests that the charge carriers involved in the *EML* of $Ba_4Si_6O_{16}:Eu^{2+}$, *RE* crystals slowly recombine with the luminescent center with time, and are thus also participating in the *LLP* at the scale of several minutes/hours.

There seems to be a strong connection between the *EML* intensity and the *LLP* intensity FIG. 9 (c). Various mechanisms were proposed to explain the mechanically-induced luminescence [29], among which those involving piezoelectricity are the most popular. It is supposed that, as a stress field is applied, the trap depths are changed thanks to piezoelectricity, ultimately altering the charge carriers recombination kinetics. Although $Ba_4Si_6O_{16}$ is centrosymmetric (space group $P2_1/c$) and should therefore not exhibit piezoelectricity, centrosymmetry might be broken at the local scale by the presence of defects, so that piezoelectricity can subsequently be observed [29]. In $Ba_2Si_2O_2N_2:Eu^{2+}$, the stress is assumed to induce a decrease of a trap depth

ACCEPTED MANUSCRIPT
The Journal of Chemical Physics
AIP Publishing
This is the author's peer reviewed, accepted manuscript. However, the online version of record will be different from this version once it has been copyedited and typeset.
PLEASE CITE THIS ARTICLE AS DOI: 10.1063/5.0167222

leading to an increased luminescence intensity [20]. In the $SrAl_2O_4:Eu^{2+}$, Dy^{3+} compound, a mechanism with three discrete traps allowed to explain an increase in the luminescence intensity both during the loading and the unloading stages [49]. This correlation is therefore consistent with this latter mechanism: a larger trap concentration with depths ranging from 0.65 to 0.85 eV is assumed i) to result in a stronger *LLP* intensity, but also ii) in a stronger *EML* intensity, as more charge carriers will be able to recombine with the luminescent center when the trap depth decreases.

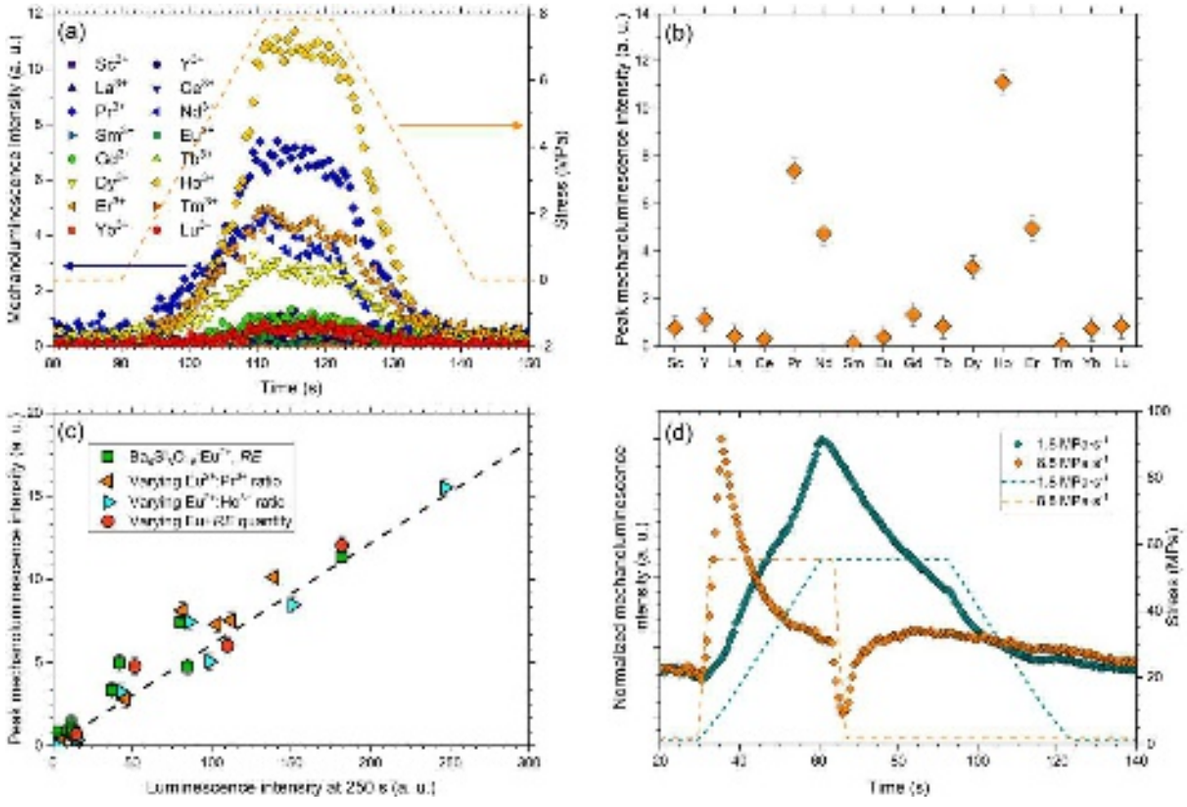

FIG. 9. (a) *EML* intensity of $Ba_4Si_6O_{16}:Eu^{2+}$, *RE*/epoxy composites (b) Peak *EML* intensity of $Ba_4Si_6O_{16}:Eu^{2+}$, *RE*/epoxy composites (c) Peak *EML* intensity plotted as a function of the luminescence intensity at 250 s (d) *EML* intensity of $Ba_4Si_6O_{16}:Eu^{2+}$, Ho^{3+}/epoxy composite with stress rates of 1.8 and 8.8 $MPa \cdot s^{-1}$.

Regarding the $Ba_4Si_6O_{16}:Eu^{2+}$, Ho^{3+} compound, its *EML* behavior contrasts with the one of $SrAl_2O_4:Eu^{2+}$, Dy^{3+}. It is particularly outlined with high stress rates (here with 8.8 $MPa \cdot s^{-1}$),

ACCEPTED MANUSCRIPT
The Journal of Chemical Physics
AIP Publishing
This is the author's peer reviewed, accepted manuscript. However, the online version of record will be different from this version once it has been copyedited and typeset.
PLEASE CITE THIS ARTICLE AS DOI: 10.1063/5.0167222

where *EML* is more intense and therefore better resolved FIG. 9 (d). It is noteworthy that the *EML* behavior of the $Ba_4Si_6O_{16}:Eu^{2+}$, Ho^{3+}/epoxy composite is identical to that of a mechanoluminescent glass-ceramic with the same cationic composition [28]. The mechanical loading and its holding lead to an increase in the luminescence intensity, while the unloading leads to a decrease of the luminescence intensity. Changes in irradiation time lead to an increase in both the luminescence and the mechanoluminescence intensity.

In particular, *TSL* experiments provide insight into the *EML* mechanism. Based on the existence of an electron trap distribution, we can propose an energy level scheme for $Ba_4Si_6O_{16}:Eu^{2+}$, Ho^{3+} FIG. 10. Although the identified charge carriers (holes and/or electrons) involved in the afterglow of $Ba_4Si_6O_{16}:Eu^{2+}$, *RE* phosphors are still unknown [32], it is assumed that electrons are the key players. Traps corresponding to the 398 K and 523 K *TSL* peaks are too deep to contribute to the *EML* effect. The Eu^{2+} ions electronic configuration changes from the ground state $4f^7$ to the $4f^65d^1$ excited state under UV light. Then, the electron can escape to the conduction band and eventually reaches energy levels located in the band gap, leaving behind Eu^{3+} ions. The main effect of the mechanical loading is to change the depth of the trap distribution, *i. e.* the C_3 and/or the C_1 trap depth decreases (FIG. 10 illustrates the scenario where the depth of the whole trap distribution decreases). The recombination probability is therefore higher and an increase of the luminescence intensity follows. However, the mechanical loading empties the stocked charge carriers at a much higher rate than it would have at rest. As a matter of fact, a smaller luminescence intensity is observed after the stress is relieved. This model provides an explanation to the observed *EML* during both mechanical loading and unloading, in consistency i) with the *EML* mechanisms involving changes in trap depths through piezoelectricity, and ii) the decrease in the *EML* intensity with long delays prior to mechanical loading in $Ba_4Si_6O_{16}:Eu^{2+}$, *RE* crystals.

ACCEPTED MANUSCRIPT
The Journal of Chemical Physics
AIP Publishing
This is the author's peer reviewed, accepted manuscript. However, the online version of record will be different from this version once it has been copyedited and typeset.
PLEASE CITE THIS ARTICLE AS DOI: 10.1063/5.0167222

ACCEPTED MANUSCRIPT
The Journal of Chemical Physics
AIP Publishing
This is the author's peer reviewed, accepted manuscript. However, the online version of record will be different from this version once it has been copyedited and typeset.
PLEASE CITE THIS ARTICLE AS DOI: 10.1063/5.0167222

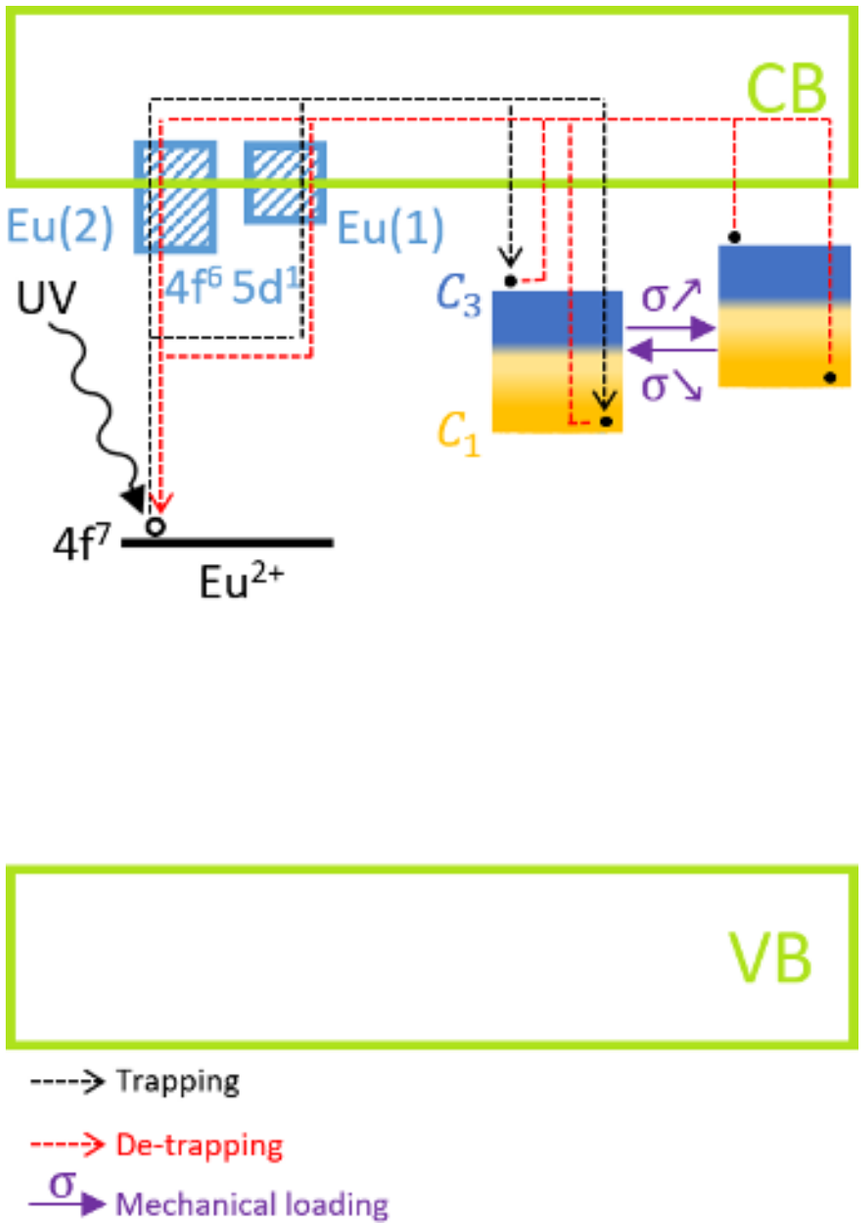

FIG. 10. Energy level scheme of $Ba_4Si_6O_{16}:Eu^{2+}$, Ho^{3+} under mechanical stress. For the sake of clarity, the trap distribution is shown as a continuous succession of trap depths.

4. CONCLUSION

The luminescence properties of $Ba_4Si_6O_{16}:Eu^{2+}$, *RE* crystals, as well as their *EML* properties, were studied. A change in the *RE* co-doping leads to small changes in the emission wavelength, but to dramatic changes in the *LLP* behavior and *EML* intensity. The incidence of the *RE*

co-doping was put into perspectives with trap depths and concentrations determined from *TSL* measurements. Exact definition of co-doping and Eu^{2+} concentration allows to tune the emission color and lifetime of $Ba_4Si_6O_{16}:Eu^{2+}$, *RE* phosphors. When *RE* = Ho^{3+}, the *LLP* duration extends beyond a day.

Emission spectra measured at low temperatures revealed a second emission band (λ_{max} = 439 nm) in addition to the green emission band (λ_{max} = 521 nm). They stem from Eu^{2+} ions located in the two non-equivalent Ba^{2+} sites in $Ba_4Si_6O_{16}$, in a similar way as in $SrAl_2O_4:Eu^{2+}, Dy^{3+}$.

TSL experiments unveiled a trap distribution from 0.694 to 0.924 eV in $Ba_4Si_6O_{16}:Eu^{2+}, Ho^{3+}$ that allowed, with *EML* experiments, to build an energy level scheme of the ongoing *EML* mechanism. Mechanical loading decreases the depth of the trap distribution, resulting in a faster release of the charge carriers and ultimately in an increase of the luminescence intensity. During unloading, the trap distribution returns to its initial position but with significantly less charge carriers, which is exhibited by a drop of the luminescence intensity *i. e.* by a negative *EML* intensity.

ACKNOWLEDGEMENTS

We acknowledge financial support from Région Bretagne and from the European Research Council (ERC Adv. Grant "DAMREG").

AUTHOR DECLARATIONS

Conflict of Interest

ACCEPTED MANUSCRIPT
The Journal of Chemical Physics
AIP Publishing
This is the author's peer reviewed, accepted manuscript. However, the online version of record will be different from this version once it has been copyedited and typeset.
PLEASE CITE THIS ARTICLE AS DOI: 10.1063/5.0167222

The authors have no conflicts to disclose.

Author Contributions

Alexis Duval: Conceptualization (lead); Data curation (lead); Investigation (lead); Methodology (lead); Writing – original draft (lead). **Yan Suffren:** Conceptualization (equal); Data curation (lead); Investigation (equal); Methodology (equal); Writing – review & editing (equal). **Mourad Benabdesselam:** Conceptualization (equal); Data curation (lead); Investigation (equal); Methodology (equal); Writing – review & editing (equal). **Patrick Houizot:** Conceptualization (equal); Investigation (equal); Methodology (equal); Supervision (equal); Writing – review & editing (equal). **Tanguy Rouxel:** Conceptualization (equal); Methodology (equal); Supervision (equal); Writing – review & editing (equal).

DATA AVAILABILITY

The data that support the findings of this study are available within the article and from the corresponding author upon reasonable request.

ORCID

Alexis Duval iD https://orcid.org/0000-0001-9192-2454

Yan Suffren iD https://orcid.org/0000-0001-6338-8274

Mourad Benabdesselam iD https://orcid.org/0000-0002-9207-2938

Patrick Houizot iD https://orcid.org/0000-0002-6360-6996

ACCEPTED MANUSCRIPT
The Journal of Chemical Physics
AIP Publishing
This is the author's peer reviewed, accepted manuscript. However, the online version of record will be different from this version once it has been copyedited and typeset.
PLEASE CITE THIS ARTICLE AS DOI: 10.1063/5.0167222

Tanguy Rouxel iD https://orcid.org/ 0000-0002-9961-245

REFERENCES

[1] X. Meng, H. Li, Z. Wang, Y. Li, H. Lin, S. Liu, and Y. He, Mater. Lett. **297**, 129928 (2021).

[2] C. Donghua, W. Hui, W. Hongjun, and Y. Weiqiang, J. Semicond. **36**, (2015).

[3] R. Zhang, T. Maeda, R. Maruta, S. Kusaka, B. Ding, K. ichiro Murai, and T. Moriga, J. Solid State Chem. **183**, 620 (2010).

[4] Z. Dong, Y. Qin, Y. Yang, D. Zhou, X. Xu, and J. Qiu, J. Rare Earths **34**, 453 (2016).

[5] P. Wang, X. Xu, D. Zhou, X. Yu, and J. Qiu, Inorg. Chem. **54**, 1690 (2015).

[6] I.S. Cho, D.K. Yim, C.H. Kwak, J.S. An, H.S. Roh, and K.S. Hong, J. Lumin. **132**, 375 (2012).

[7] Y. Li, Y. Fang, N. Hirosaki, R.J. Xie, L. Liu, T. Takeda, and X. Li, Materials (Basel). **3**, 1692 (2010).

[8] M. Chen, Z. Xia, M.S. Molokeev, and Q. Liu, J. Mater. Chem. C **3**, 12477 (2015).

[9] W.-S. Song, H.-J. Kim, Y.-S. Kim, and H. Yang, J. Electrochem. Soc. **157**, J319 (2010).

[10] Z. Yang, Y. Hu, L. Chen, and X. Wang, Opt. Mater. (Amst). **35**, 1264 (2013).

[11] Y. Jia, W. Sun, R. Pang, T. Ma, D. Li, H. Li, S. Zhang, J. Fu, L. Jiang, and C. Li, Mater. Des. **90**, 218 (2016).

[12] X. Li, Y. Liang, F. Yang, Z. Xia, W. Huang, and Y. Li, J. Mater. Sci. Mater. Electron. **24**, 3199 (2013).

ACCEPTED MANUSCRIPT
The Journal of Chemical Physics
AIP Publishing
This is the author's peer reviewed accepted manuscript. However, the online version of record will be different from this version once it has been copyedited and typeset.
PLEASE CITE THIS ARTICLE AS DOI: 10.1063/5.0167222

ACCEPTED MANUSCRIPT
The Journal of Chemical Physics
AIP Publishing
This is the author's peer reviewed, accepted manuscript. However, the online version of record will be different from this version once it has been copyedited and typeset.
PLEASE CITE THIS ARTICLE AS DOI: 10.1063/5.0167222

[13] M. Zhang, J. Wang, Q. Zhang, W. Ding, and Q. Su, **42**, 33 (2007).

[14] D. Kim, T.H. Kim, T.E. Hong, J. Bae, C.H. Kim, J. Kim, S. Kim, K. Jeon, and J. Park, Materials (Basel). **13**, 1859 (2020).

[15] K. Asami, J. Ueda, K. Yasuda, K. Hongo, R. Maezono, M.G. Brik, and S. Tanabe, Opt. Mater. (Amst). **84**, 436 (2018).

[16] M. Yamaga, Y. Masui, S. Sakuta, N. Kodama, and K. Kaminaga, Phys. Rev. B - Condens. Matter Mater. Phys. **71**, 1 (2005).

[17] M. Yamaga, Y. Masui, and N. Kodama, Opt. Mater. (Amst). **36**, 1776 (2014).

[18] J.K. Park, M.A. Lim, K.J. Choi, and C.H. Kim, J. Mater. Sci. **40**, 2069 (2005).

[19] S.H. Choi, S. Bin Kwon, U. Bin Humayoun, W.K. Park, K. Toda, M. Kakihana, T. Masaki, W.S. Yang, Y.H. Song, and D.H. Yoon, Dye. Pigment. **148**, 460 (2018).

[20] J. Botterman, K. Van Den Eeckhout, I. De Baere, D. Poelman, and P.F. Smet, Acta Mater. **60**, 5494 (2012).

[21] H. Pan, D. Luo, L. Wang, and Y. Li, Int. Conf. Manuf. Sci. Eng. (ICMSE 2015) 690 (2015).

[22] B. Wang, J. Chen, Y. Xia, and Y. Liu, J. Nanosci. Nanotechnol. **16**, 3608 (2016).

[23] P.F. Smet, J. Botterman, K. Van Den Eeckhout, K. Korthout, and D. Poelman, Opt. Mater. (Amst). **36**, 1913 (2014).

[24] F. Xiao, Y.N. Xue, and Q.Y. Zhang, Spectrochim. Acta - Part A Mol. Biomol. Spectrosc. **74**, 758 (2009).

[25] W. Peng-Jiu, X. Xu-Hui, Q. Jian-Bei, Z. Da-Cheng, L. Xue-E, and C. Shuai, Acta Phys.

ACCEPTED MANUSCRIPT
The Journal of Chemical Physics
AIP Publishing
This is the author's peer reviewed, accepted manuscript. However, the online version of record will be different from this version once it has been copyedited and typeset.
PLEASE CITE THIS ARTICLE AS DOI: 10.1063/5.0167222

Sin. **63**, 077804 (2014).

[26] R.D. Shannon, Acta Crystallogr. Sect. A **32**, 751 (1976).

[27] K.-F. Hesse and F. Liebau, Zeitschrift Für Krist. **153**, 3 (1980).

[28] A. Duval, P. Houizot, X. Rocquefelte, and T. Rouxel, Appl. Phys. Lett. **123**, 011905 (2023).

[29] A. Feng and P.F. Smet, Materials (Basel). **11**, 484 (2018).

[30] C. Lara, M.J. Pascual, and A. Durán, J. Non. Cryst. Solids **348**, 149 (2004).

[31] N. Claussen and J. Jahn, Powder Metall. Inernational **2**, 87 (1970).

[32] Y. Gong, Y. Wang, Y. Li, X. Xu, and W. Zeng, Opt. Express **19**, 4310 (2011).

[33] P. Wang, X. Xu, J. Qiu, X. Yu, and Q. Wang, Opt. Mater. (Amst). **36**, 1826 (2014).

[34] G.H. Dieke and H.M. Crosswhite, Appl. Opt. **2**, 675 (1963).

[35] J. Ueda, Bull. Chem. Soc. Jpn. **94**, 2807 (2021).

[36] A. Nag and T.R.N. Kutty, J. Alloys Compd. **354**, 221 (2003).

[37] J. Botterman, K. Van den Eeckhout, A.J.J. Bos, P. Dorenbos, and P.F. Smet, Opt. Mater. Express **2**, 341 (2012).

[38] R. Chen and Y. Kirsh, Int. Ser. Sci. Solid State **15**, 17 (1981).

[39] R. Chen, J. Electrochem. Soc. **116**, 1254 (1969).

[40] M.S. Jahan, D.W. Cooke, W.L. Hults, J.L. Smith, B.L. Bennett, and M.A. Maez, J. Lumin. **47**, 85 (1990).

[41] J.T. Randall and M.H.F. Wilkins, Proc. R. Soc. London. Ser. A. Math. Phys. Sci. **184**, 365

(1945).

[42] J.T. Randall and M.H.F. Wilkins, Proc. R. Soc. London. Ser. A. Math. Phys. Sci. **184**, 390 (1945).

[43] W.F. Hornyak and R. Chen, J. Lumin. **44**, 73 (1989).

[44] W.L. Medlin, Phys. Rev. **123**, 502 (1961).

[45] X. Zhang, X. Xu, Q. He, J. Qiu, and X. Yu, ECS J. Solid State Sci. Technol. **2**, R225 (2013).

[46] G. Blasse and B.C. Grabmaier, Springer (1994).

[47] J. Botterman, J.J. Joos, and P.F. Smet, Phys. Rev. B - Condens. Matter Mater. Phys. **90**, 1 (2014).

[48] M. Dubernet, Y. Gueguen, P. Houizot, F. Célarié, J.C. Sangleboeuf, H. Orain, and T. Rouxel, Appl. Phys. Lett. **107**, 151906 (2015).

[49] M. Dubernet, E. Bruyer, Y. Gueguen, P. Houizot, J.C. Hameline, X. Rocquefelte, and T. Rouxel, Sci. Rep. **10**, 19495 (2020).

ACCEPTED MANUSCRIPT
The Journal of Chemical Physics
AIP Publishing
This is the author's peer reviewed, accepted manuscript. However, the online version of record will be different from this version once it has been copyedited and typeset.
PLEASE CITE THIS ARTICLE AS DOI: 10.1063/5.0167222